

## Polarized Nuclear and Atomic Systems

Jahan Singh

*Department of Physics, Maharshi Dayanand University, Rohtak, India*

(Revised manuscript received October 1, 1991)

A review of the basic principles, status and methods for the production of polarized systems is presented. The performance of different techniques is compared and new developments are described. It is shown that the schemes for many kinds of polarized ions exist. The prospects for further improvements and development of all types of polarized systems are encouraging.

### I. INTRODUCTION

During the last thirty years a large amount of research in Atomic and Nuclear Physics has been conducted in theoretical and experimental aspects of spin orientation techniques. It is well recognized that the experiments with polarized systems can reveal much information of the composition of the systems and the interactions of sub-systems. Many laboratories have developed the polarized systems and had measured the polarization and asymmetries using these polarized systems. The development and experiments with polarized systems have been reviewed at six International Symposia<sup>1</sup> held at Basel (1960); Karlsruhe (1965); Madison (1970); Zurich (1975); Santa Fe (1980) and Osaka (1985) and some other workshops and Symposia<sup>7-15</sup>. In the present talk an attempt has been made to give an elementary treatment of the polarization effects in the Atomic and Nuclear systems. The latest developments after the Sixth International symposium on Polarization Phenomena in Nuclear Physics held at Osaka in 1985 and recently developed Heavy Ion polarized sources are described in detail.

### II. POLARIZED SYSTEMS

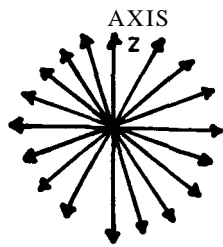
Normally in a target or in a beam, the spin axes of the particles (atoms/Nuclei) point in all directions and randomly. These types of systems are called "Unoriented (Unpolarized)" assemblies. Many elegant experiments can be devised and new effects are observed if the spin axes of the particles are made parallel to a certain direction called as the quantization axis. If we consider a system of having spin ' $I$ ' is placed in an external magnetic field then the particles can be in any one of  $(2I + 1)$  "orientation states" which are characterized by the magnetic quantum Numbers ' $m$ '. If all the orientation states have the same "occupational number" then the system is called unpolarized assembly. On the other hand if the occupation number for the different

states are unequal, the system is called "oriented assembly" as shown in Fig. 1. The polarized systems are of two types:

**11-1. Vector Polarized Assembly**

When the occupation number for the positive and negative values of the same magnetic quantum number are unequal then the system is called "Vector Polarized". The degree of polarization is defined by a parameter:

UNPOLARISED  
( $1 \neq 0$ )

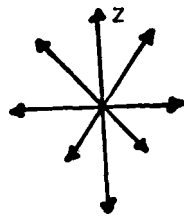


OCCUPATION NO = LENGTH OF ARROWS

EQUAL LENGTHS  
 $N_{+m} = N_{-m}$   
ALSO  $N_m(I) = N_m(J)$

( $2I + 1$ ) STATES HAVE EQUAL NO. PARTICLES

VECTOR POLARISED



THE OCCUPATION NO FOR +m AND -m ARE UNEQUAL  
 $N_{+m} \neq N_{-m}$

VECTOR POLARIZATION (DEGREE OF POLARIZATION)

$$P_i = \frac{\sum_m m \cdot N_m}{I \cdot \sum_m N_m} \quad \text{WHERE } i = 1, 2, 3.$$

SPIN -1/2 NUCLEI e.g. ( $\frac{1}{2}H$ )  
 $m = +1/2$  or  $m = -1/2$

OCCUPATION NOS  $N_+$  AND  $N_-$ . 
$$P = \frac{N_+ - N_-}{N_+ + N_-} = N_+ - N_-$$

NORMALIZATION GIVE-S  $N_+ + N_- = 1$   
THUS P HAS VALUES BETWEEN +1 AND -1

TENSOR POLARISED



$N_{-t-m} = N_{-m}$   
BUT  
 $N_m(i) \neq N_m(j)$

FIG. 1. Representation of unpolarized and polarized systems.

$$P = \frac{\sum m \cdot N_m}{I \cdot \sum N_m} \quad (1)$$

where  $N_m$  is the population of orientation states for magnetic quantum number "m", For the dis-oriented assembly, the population of states for + m and -m are equal i.e.  $N_m = N_{-m}$  and  $P = 0.0$ .

For the polarized assembly  $N_m \neq N_{-m}$  and have the possibilities:

- (i) either  $N_m = 0$  or  $N_{-m} = 0$ . This gives  $P = -1.0$  or  $+1.0$  because  $\sum N_m = 1$ .
- (ii) There is a mixture of  $N_m$  and  $N_{-m}$ . Then  $P$  lies between  $+1$  and  $-1$  i.e.  $1 \geq P \geq -1$ .

## II-2. Tensor Polarized Assembly (Aligned Assembly)

If the particles are oriented along the quantization axis such that  $N_m = N_{-m}$  but  $N_m(i) \neq N_m(j)$  where 'i' and 'j' denote the indices for the different quantum numbers of the spin operator. There are more particles in one direction than the other. For such systems the degree of orientation (alignment) called "Tensor Polarization" is defined by the parameter:

$$P_{ij} = 3 \left[ \sum N_m \cdot \left\{ m^2 - I(I+1)/3 \right\} \right] / I^2 \cdot \sum N_m \quad (2)$$

It should be noted that  $P_{ij} = 0$  for the system having the spin less than one. In terms of the above parameters  $P$  and  $P_{ij}$  we have the following systems:

- (i)  $P = 0 = P_{ij}$  for a disoriented assembly;
- (ii)  $P \neq 0$  but  $P_{ij} = 0$  for a pure vector Polarized Assembly;
- (iii)  $P \neq 0$  and  $P_{ij} \neq 0$  for the mixed vector and tensor assembly and
- (iv)  $P = 0$  but  $P_{ij} \neq 0$  for a pure tensor assembly.

## III. MEASUREMENT WITH POLARIZED SYSTEMS

There are, in general, two types of polarization measurements, Firstly, the polarization measurements in which an initially unpolarized beam is scattered from the target under investigation and polarization produced is subsequently analysed by a target of known polarization efficiency. Secondly, the asymmetry measurements in which the polarized beam is used to measure asymmetries in the scattering from the target in question. These two quantities are identical for elastic scattering due to the invariance of the scattering under time reversal but the two quantities are not identical for de-excitation and inelastic scattering. These measurements are shown in Fig. 2 and are summarised below:

- (i) when an unpolarized beam is incident on the target then equal number of the nuclei are scattered to the left and right sides but each side has a different number of the spin up and spin down nuclei. Hence, the scattered beam is polarized i.e. target acts as a polarizer, we define

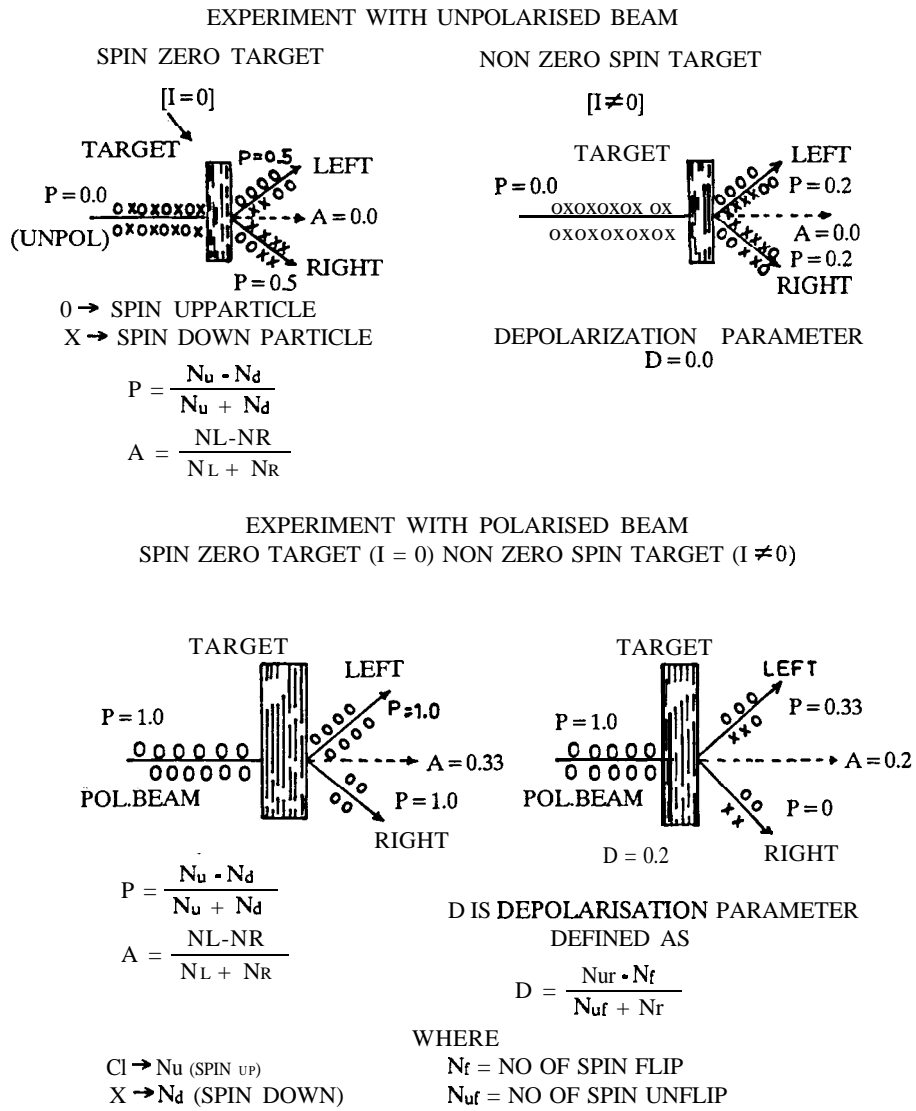


FIG. 2. Experiments with Polarized beams.

the polarizing power as:

$$P = (N_u - N_d) / (N_u + N_d) \tag{3}$$

Where  $N_u$  and  $N_d$  are the number of the particles with spin up and spin down in the same side.

(ii) If a completely polarized beam is scattered by the spin zero target then more nuclei are scattered to the left or right side depending upon the direction of beam polarization. We measure the asymmetry parameter (called the analyzing power) defined as:

$$A = (N_L - N_R)/(N_L + N_R) \quad (4)$$

Where  $N_L$  and  $N_R$  are the numbers of particles scattered to the left and right sides respectively, Hence, the target acts as analyzer.

(iii) When the polarized beam is scattered with the target having non-zero spin, then it is possible for a nucleus with spin in one direction to have its spin flipped into the opposite direction in the scattering process. The change in angular momentum due to the spin flip can be taken up by the target nucleus if it has a spin. The probability of the spin flip is defined by a depolarization parameters.

$$D = (N_{uf} - N_f)/(N_{uf} + N_f) \quad (5)$$

Where  $N_{uf}$  and  $N_f$  are the number of the scattered nuclei without and with spin flip to either side respectively. The depolarization parameter can be used to study the spin behaviour of the target nucleus.

(iv) In this method the unknown forms the first target and the scattered beam is analysed at a second scattering. The asymmetry produced at the second scattering is given in terms of the numbers of the particles scattered to the left and to the right as:

$$A = (N_{RR} - N_{RL})/(N_{RR} + N_{RL}) \quad \text{or} \quad A = (N_{LL} - N_{LR})/(N_{LL} + N_{LR}) \quad (6)$$

depending on whether the first scattering is to the left or to the right of the incident beam. If the two scatterings are coplaner then the asymmetry can be written as:

$$A = P_1 \cdot P_2 \quad (7)$$

Where  $P_1$  and  $P_2$  are the polarization produced at the first and second scattering respectively. Experimentally, the asymmetry is determined by Eq. 6 and from the known value of  $P_2$ , the  $P_1$  is calculated using Eq. (7).

The polarization measurements allows:

- (i) the determination of few-nucleon wave function;
- (ii) the search of symmetry law violations in Nucleon-Nucleon interactions;
- (iii) to find the strength of the spin-orbit interactions;
- (iv) to study the nature of nuclear forces;
- (v) the separation of direct interaction and compound nuclear contributions in the nuclear reactions.
- (vi) to find the angular momentum transfer in the interactions;
- (vii) to study the spin behaviour of the target system.
- (viii) to test the time reversal invariance by the comparison of the quantity  $P_y - A_y$  in  $P\text{-}^3\text{He}$  and  $P\text{-}^3\text{H}$  elastic scattering.

and

(ix) to find the parity non-conservation in strong interaction.

Recently, the parity-violation of proton-proton scattering at 6 Ge V/C has been examined in a relationized meson exchange by Henley.<sup>16</sup> For the above cited applications we require the precision measurements of the vector and tensor analysing powers using the polarized beams and polarized targets.

#### IV. PRODUCTION OF POLARIZED TARGETS

The methods used for orientation of the systems at rest can be classified into two main categories-Thermal equilibrium methods; Non-thermal equilibrium or steady state methods. We shall discuss in brief the above categories:

##### IV-1. Thermal Equilibrium Methods

These methods are based on the idea that some kind of interaction produces hf splitting of the nuclei which are to be oriented and the specimen is cooled to such a temperature (0.01 to 0.1 K) that only the lower of the hf levels are appreciably populated. The chosen lowest hf levels correspond to a spatial orientations nuclei. The hf splitting is obtained by the magnetic hyperfine structure (Brute Force method) or The electric hyperfine structure (Pound's method). In the later method the interaction between the nuclear electric quadrupole moment and the electric field gradient is produced by the electrons around the nucleus causes a hf splitting. This method produces alignment but no polarization. The symmetry axis (z axis) is determined by the position of the electrons.

A useful alignment at accessible low temperature is possible only when the nucleus has a large quadrupole moment and when the field gradient is produced by the valence electrons of the atom in which the nucleus is situated. Thus, this method is limited to heavy nuclei whose atoms have the correct chemical properties. Using this method Dabbs<sup>17</sup> et al had oriented the odd Uranium isotopes in  $\text{UO}_2\text{Rb}(\text{NO}_3)_3$  at 1°k.

##### W-2. Non-thermal Equilibrium Methods of Nuclear Orientation

Nuclear orientation is a consequence of unequal population of the spin orientation states. The populations of the different states can be changed by inducing transitions between them with electromagnetic radiation; microwaves and Lasers. The nuclear orientation so produced can be maintained if either; The time needed for the nuclei to come to equilibrium with the lattice happens to be long. These are so called "transient methods" . OR the radiation which causes the transition is maintained continuously, and the system comes to a non-thermal equilibrium steady state. These are called "dynamic methods" . A mechanism which changes the populations of two levels increasing one at the expense of the other is called a pumping mechanism. In general, the following three pumping devices are used:

## (i) Microwave pumping

The system in which the nuclei are to be polarized should contain free electron spins (provided by impurities, free radicals, conduction electrons etc.) A magnetic field  $B_0$  is applied to separate the levels of the electron spins so that the microwave field can induce transitions between them. The temperature of the system is chosen so that in thermal equilibrium in the field  $B_0$ , the populations of the electron spin levels are appreciably unequal. The microwave field is applied to the system to separate the transition between the electron spin levels. At least one nucleus is coupled to each electron spin, and if the system has been correctly chosen, the nuclei become polarized when the electron spin transition is saturated. This is done either as Overhauser effect<sup>18</sup> or as Abragaon Jeffries effect.” The change in populations of the levels by applied microwave field is consistent with the principle of minimum production of entropy. From an experimental point of view, three conditions must be simultaneously satisfied in order successfully to produce large nuclear polarizations by microwave pumping.

(1) The separation between the Zeeman levels of the electron spin must be such that it may be produced by a field easily available, and that transitions between the levels are induced by an available source of microwave.

(2) The temperature must be so low that, with the Zeeman splitting chosen, the electron spin polarization is large enough, since the nuclear polarization achieved will be of the same order of magnitude. The temperature must also be easily available.

(3) The relaxation times must be sufficiently long that the transitions may be saturated with a reasonable amount of available microwave power.

The above conditions are satisfied for the frequency of 34 kHz and the temp. of 1° K.

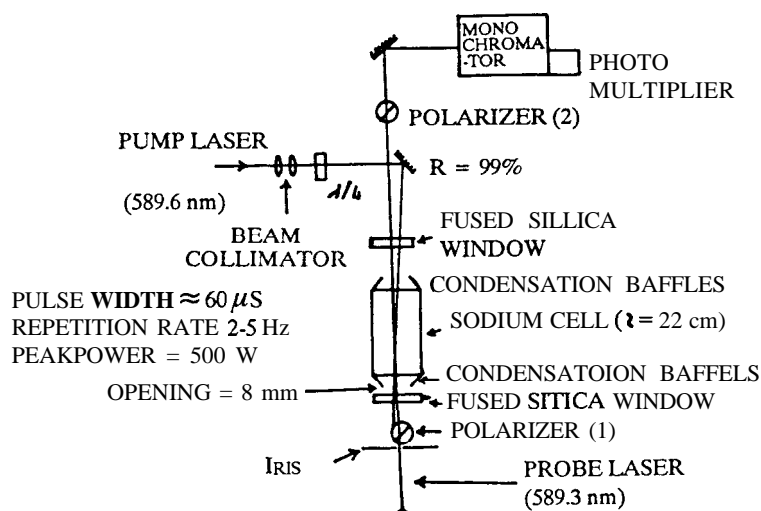
## (ii) Optical Pumping

The use of visible light to orient atomic or nuclear spins had been reviewed by Kastler.<sup>20</sup> It can be explained for the sodium atoms which emit 589.593 nm ( $D_1$ ) and 588.996 nm ( $D_2$ ) among other wavelengths. These lines correspond to transitions from the first excited states  $2P_{1/2}$  and  $2P_{3/2}$  to the ground state  $2S_{1/2}$ . In a magnetic field ( $B_0$ ) they are split into 10 components (anomalous Zeeman effect). The same radiation which is emitted by the excited atoms is absorbed by ground state atoms to produce that excited state. When the sodium vapour is irradiated with R.H.C.P. light of  $D_1$  Wavelength in the direction of applied magnetic field.  $B_0$  ( $\sigma^+$  lines) then the sodium atoms in the ground state with  $m = -1/2$  will be excited into the  $2P_{1/2}$  state with  $m = +1/2$ . They will then decay back to the ground state by spontaneous emission of radiation by two equally probable path (half will go to the ground state with  $m = +1/2$  and half will go to the ground state with  $m = -1/2$ ). The latter will be excited again by the incoming radiation so that the net result of this process is that sodium atoms are transferred from the ground state with  $m = -1/2$  to the ground state with  $m = +1/2$ . If there is no mechanism for sodium atoms in the ground state to go from the  $m = +1/2$  level to the  $m = -1/2$  level, the sodium atoms will be polarized.

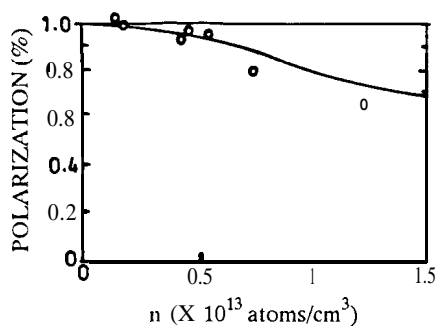
The technique of optical pumping has been successfully utilized to obtain the polarization of the odd mercury isotopes by Cagnae et al,<sup>21</sup> for the polarized  $^3\text{He}$  target by Hardy et al<sup>22</sup> and optically Pumped Polarized ion source by York et al<sup>23</sup> respectively.

(iii) Laser Pumping

One of the principal difficulties encountered in optical pumping has been to get sufficient power in the incident light beam. Therefore, recently at KEK, Japan,<sup>24-26</sup> the electron-spin polarized sodium atoms have been produced by optical pumping with two single frequency dye lasers tuned to the wavelength of the sodium  $D_1$  (589.593 nm) line. The electron spin-polarization is strongly affected by the laser power and the sodium target density. When two pumping lasers were used, a sodium electron-spin polarization of about 90% was obtained at a target thickness of  $1 \times 10^{13} \text{ n/cm}^2$ . The experimental set-up for the optical pumping and polarization of alkali atoms with intense laser light is shown schematically in Fig. 3.



(a) EXPERIMENTAL SETUP FOR OPTICALLY PUMPED Na TARGET



(b) SODIUM POLARIZATION AS A FUNCTION OF TARGET THICKNESS.

FIG. 3. Laser pumping of sodium atoms

## V. PRODUCTION OF POLARIZED ION BEAMS (POLARIZED ION SOURCES)

The Polarized Ion beams can be produced either by the scattering of unpolarized beam from the targets OR by the polarized Ion sources (PIS). While the scattering from the target is attractive in its simplicity and has been able to provide polarized beams for many experiments but the polarized ion sources are undoubtedly better and have many advantages as: higher intensity; control of polarization mode and direction; freedom from first scattered radiation which may block or produce undesirable background in the detectors as double scattering is used; energy resolution and beam emittance are good and the variation of energy of the polarized beam is easier.

The construction of PIS is complex and expensive but their operational advantages justify the expense and complication of building the polarized ion source. Therefore, many laboratories in the world have developed PIS for electrons, protons, deuterons,  $^3\text{He}$  and heavy ions. In this review paper the basic principles and recent developments in the polarized ion sources' design and technology are described. At present, an increasing variety of methods for the production of polarized atoms and ions have been used, the methods for the product of polarized ions can be classified as: Ground state atomic beam sources (Conventional atomic beam method); polarized ion sources based on metastable atoms (Lamb shift sources) and Production of Polarized Atoms by spin exchange collisions (Optically pumped sources).

All production methods for the polarized ions have in common that at first a polarized neutral atomic beam is prepared, which subsequently is ionized selectively to produce positive or negative ions. The distinction between the different types of sources is based on the method by which the neutral beam is produced and polarized and the process used to ionize the neutral atoms (the electron bombardment, charge transfer and charge exchange).

### V-1. Ground State Atomic Beam Sources

A schematic diagram of the conventional atomic beam source is shown in Fig. 4. Hydrogen or deuterium atoms are generated by dissociation of molecules in a R.F. or Microwave discharge. An atomic beam of thermal velocity is formed by a single hole (multichannel collimator, nozzle) and Skimmer. This atomic beam is passed through an inhomogeneous sextupole magnetic field. This Stern-Gerlach separation magnetic field interacts with the magnetic moment of the atoms. Depending upon the direction of atomic magnetic moment either parallel or anti-parallel to the applied field the atoms are focussed towards the axis or defocussed away from the axis. Hence, the sextupole magnetic field delivers a fully electron polarized atomic beam. Then this electron polarized beam is passed through R.F. transition unit which can change the population of the magnetic substates. Thus, the application of R.F. transitions between hyperfine substates of the atoms selects different nuclear polarization and provides rapid spin reversal. This nuclear

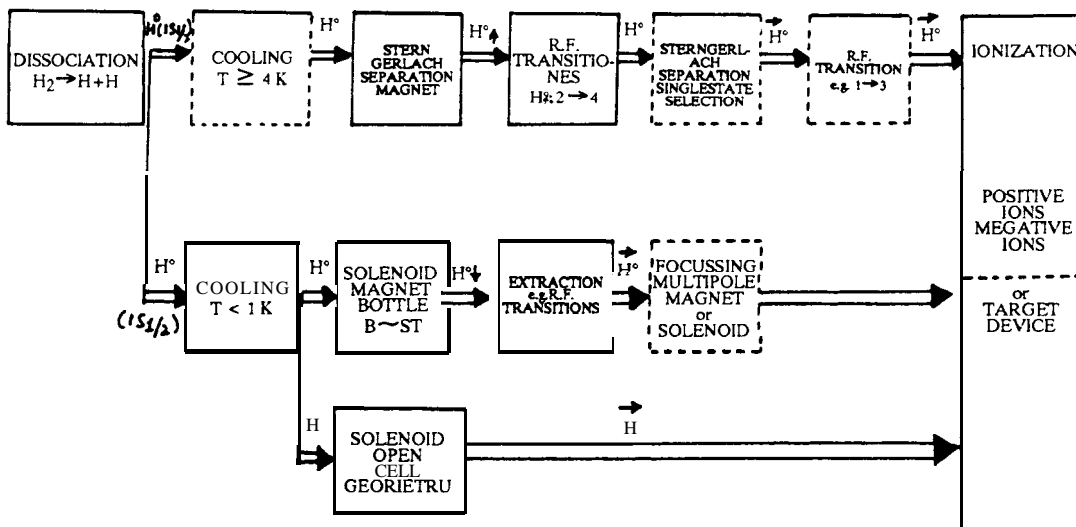


FIG. 4. Schematic diagram of atomic beam source.

polarized neutral beam can be used as a nearly 100% polarized hydrogen jet target or can be compressed in a vessel. For polarized ions the atoms are converted to positive or negative ions

TABLE I. Production of Polarized Atomic Deuterium Beams

Mode	Ionizer or target B-field	Stern-Gerlach (S-G) and rf-transitions	Substates	Vector pol.pz	Tensor pol.pzz	Relative intensity I	Figure of Merit $I \cdot p_z^2$	Figure of Merit $I \cdot p_z^2 p_{zz}^2$
a	strong	S-G	1+2+3	0	0	1	0	0
b	strong	S-G 1→4 (WF)	2+3+4	-2/3	0	1	4/9	0
c	strong	S-G 2→6 3→5	1+5+6	+2/3	0	1	4/9	0
d	strong	S-G 3→5	1+2+5	+1/3	-1	1	1/9	1
e	strong	S-G 1→4 3→5 2→3 5→6 (WF)	3+4+6	-1/3	+1	1	1/9	1
f	stomg	S-G 2→6	1+3+6	+1/3	+1	1	1/9	1
g	stomg	S-G 2→6 3→2 6→5 (WF)	2+4+5	-1/3	-1	1	1/9	1
h	strong	S-G 1→4 (WF) S-G 3→5	2+5	0	-2	2/3	0	8/3
i	strong	S-G 1→4 (WF) S-G 2→6	3+6	0	+1	2/3	0	2/3
k	strong	S-G 3→5 S-G 2→6	1+6	+1	+1	2/3	2/3	2/3
l	strong	S-G 3→5 S-G 1→4 (WF) 2→3	3+4	-1	+1	2/3	2/3	2/3
m	any	S-G 2→6 S-G 3→4	1+4	0	+1	2/3	0	2/3
n	any	S-G 3→5 2→6 S-G	1	+1	+1	1/3	1/3	1/3
o	any	S-G 3→5 2→6 S-G 1→4 (WF)	4	-1	+1	1/3	1/3	1/3

Strong 6-field: >> 117 Gauss

by different processes. This simple conventional scheme had been used in many operational polarized ion sources since 1960 producing polarized  $H^+$  and  $D^+$  beams. A representation diagram of the polarized atomic beam sources used at Birmingham is shown in Fig. 5. The intensity of the polarized ion beams obtained from atomic beam sources depends upon the parameters: (1) the initial gas input rate into the dissociator, (2) the degree of dissociation, (3) the atomic effusion device at the exit of the dissociator, (4) the solid angle of acceptance of the sextupole magnet and its separation efficiency for parallel and anti-parallel electron spins, (5) the transition efficiency of R.F. transitions, (6) the ionization efficiency, (7) the injection and ex-

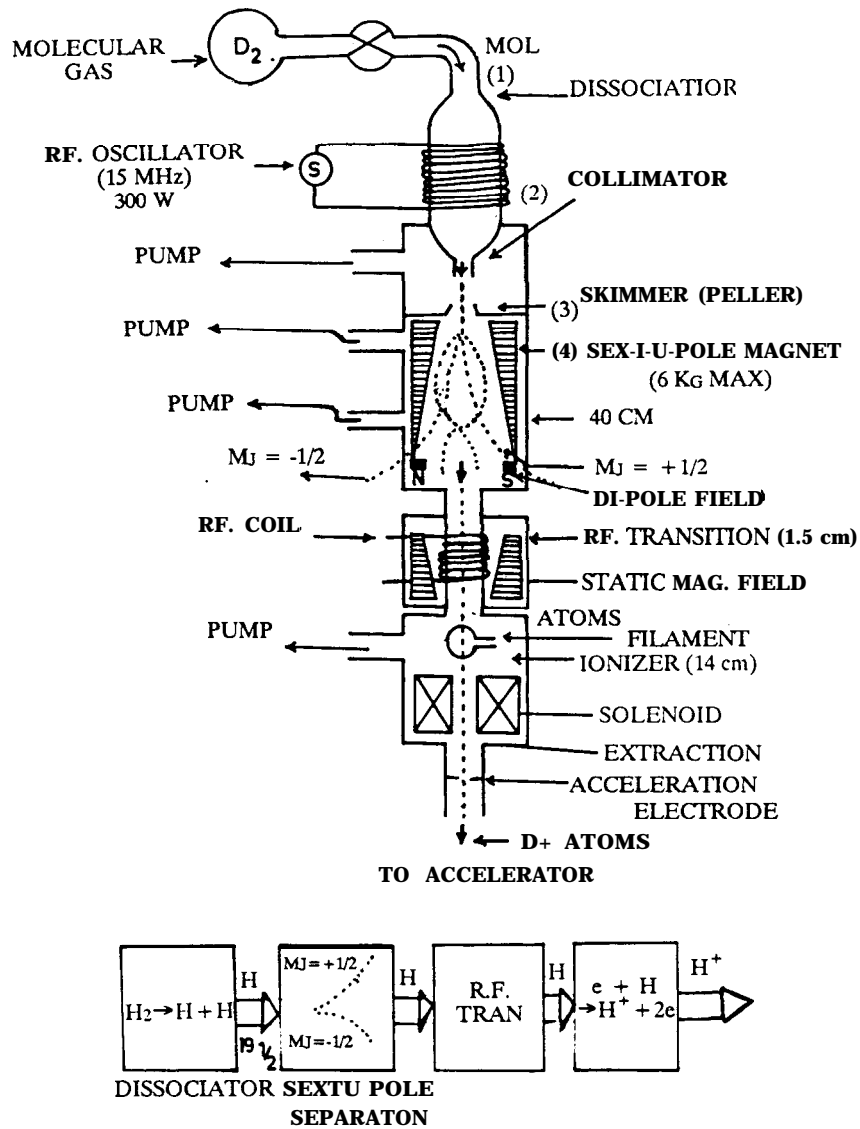


FIG. 5. Birmingham Polarized Deuteron Source (PDS).

traction efficiencies of the systems used at the accelerator and (8) the atomic beam scattering. The substantial advances have been made in the intensity of polarized proton and deuteron beam obtained from the atomic beam sources since 1960 as shown in Fig. 6. This progress can be attributed to the improvement in the design of the various components of the atomic beam such as **ionization of atomic beams**: having obtained an atomic beam containing the required states of the atom it is necessary to ionize the sufficiently large fraction of this beam without any serious loss of nuclear polarization and without adding a too large flux of upolarized nuclei (it arises due to ionization of residual gas). The polarized ion beam must also be produced with a size and **emittance** which is acceptable to the accelerator. The efficiency of the ionizer must

POLARIZED H<sup>+</sup> AND D<sup>+</sup> BEAMS

1960	0.1 $\mu\text{A}$
1965	1.0 $\mu\text{A}$
1972	10 $\mu\text{A}$
197s	30 $\mu\text{A}$
1976	60 $\mu\text{A}$
1977	70 $\mu\text{A}$
1980	100 $\mu\text{A}$
1985	100 $\mu\text{A}$
1988	100 TO 1000 $\mu\text{A}$ (-1 TO 1 mA)

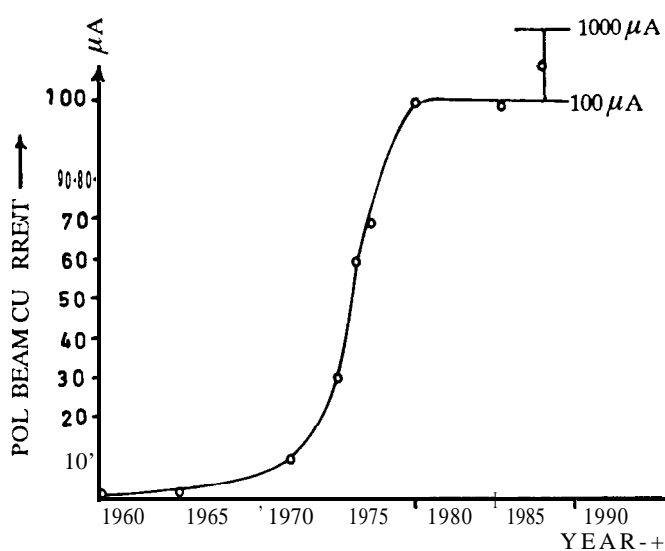


FIG. 6. Polarized Atomic beam intensity versus the years.

be high enough to produce a final accelerated beam intensity which is sufficient for the experiments envisaged. Mostly PIS use the electrom bombardment ionizer. To evaluate the performance of an ionizer it is necessary to know the ionization cross-sections for the atoms in the beam and the atoms of the residual gas, the electron currents, the ion extraction efficiency and emittance and the magnitude of depolarizing effects. The different used and proposed ionization processes are collected in Table II.

TABLE II. Ionization Processes

Process	$\sigma$ (cm <sup>2</sup> )	Intensity relation for a conventional atomic BEAM $I(H \rightarrow H^+) = 2 \cdot 10^{16} S^{-1} cm^{-2}$ $V_0 = 3 \cdot 10^7 cm S^{-1} n \approx 10^{11} cm^{-3}$	Ionizing Beam Intensity [ $\mu A/cm^2$ ]	$I(H_{ion})$ (125)	$I(H_{ion})$ special Conditions (cooled Atomic beam, pulsed etc.) ( $\mu A$ )	$I(H_{ion})$ Corresponding DC-beam ( $\mu A$ )
(1) $\bar{H}^0 + e^- \xrightarrow{1KeV} \bar{H}^+ + 2e^-$	$0.7 \cdot 10^{-16}$	$I @ + \approx 0.05 \mu A$ per mA/cm <sup>2</sup> e <sup>-</sup>	$2.5 \cdot 10^3$	125	500 <sup>(a)</sup>	50
(2) $\bar{H}^0 + D^+ (+, e^+) \xrightarrow[space\ charge\ compensation]{2KeV} \bar{H}^+ + D^0 (+, e^-)$	$20 \cdot 10^{-16}$	$I(\bar{H}^+) \approx 5 \mu A$ per mA/cm <sup>2</sup> H+	100		10000 <sup>(b)</sup>	0.5
(3) $\bar{H}^0 + C_6 \xrightarrow[KeV]{50} \bar{H}^+ + C_6^+$	$6 \cdot 10^{-16}$	$I(\bar{H}^+) \approx 15 \mu A$ per mA/cm <sup>2</sup> C <sub>6</sub> <sup>+</sup>	2	3	30 <sup>(c)</sup>	0.015
(4) $\bar{H}^0 + D^+ (+, CS^+) \xrightarrow[KeV]{2} \bar{H}^+ + D^0 (+, CS^+)$ ↑ space charge compensation ↑	$20 \cdot 10^{-16}$	$I(\bar{H}^+) \approx 5 \mu A$ per mA/cm <sup>2</sup> D <sup>+</sup>	2			
(5) Process 1) + $\bar{H}^0 + Na^+ \xrightarrow[n=5\%]{0.5KeV} \bar{H}^+ + Na^+$	$3 \cdot 10^{-16}$	$I(\bar{H}^+) \approx 0.003 \mu A$ per mA/cm <sup>2</sup> e <sup>-</sup>	$2.5 \cdot 10^3$	6	25 <sup>(d)</sup>	25

(a) dc beam, Cooled atomic beam (accommodator T = 35K) ∈ THZ

(b) Pulsed peak current, average current during 100μs = 5mA, repetition rate 1Hz, cooled atomic beam, nozzle cooling with LN<sub>2</sub> (MOSCOW)

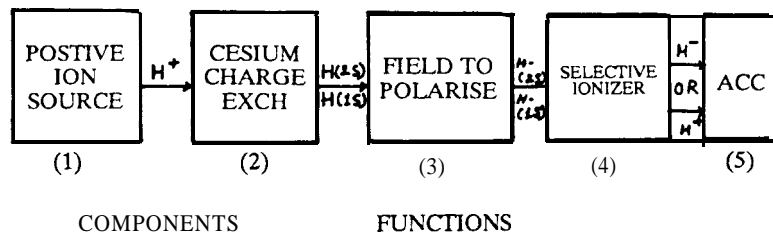
(c) Pulsed peak current during 100μs, repetition rate 1Hz, cooled atomic beam, nozzle cooling (Brookhaven)

## V-2. Polarized Ion Sources Based on Metastable Atoms (Lamb-Shift Sources)

The general Lamb-Shift scheme is shown in Fig. 7. The protons obtained from either a R.F. ion source, a duoplasmatron or ECR ionizer, pass through a cesium charge exchange canal where a substantial fraction is converted into metastable 2S<sub>1/2</sub> atoms. The charge components emerging from the cell are deflected out of the neutral beam by electrostatic deflector plates. The metastable atoms in the beam are polarized by eliminating the undesired spin states by transitions from a 2S<sub>1/2</sub> state to a 2P<sub>1/2</sub> state induced either by static fields or a combination of static fields or a combination of static and rf fields. The 2P<sub>1/2</sub> state decays spontaneously to the 1S<sub>1/2</sub> ground state. After this spin-state selection the metastable beam is selectively ionized by passing the beam through Argon gas for negative ions and iodine vapour for positive ions. A description of the Lamb-shift polarized ion source installed on a Tandem accelerator had been given by Clegg et al.<sup>27</sup>

After the construction of the above source at university of Wisconsin, the Lamb-shift sources have been well investigated in many laboratories and many sources have been operational

## LAMB-SHIFT POLARISED ION SOURCE



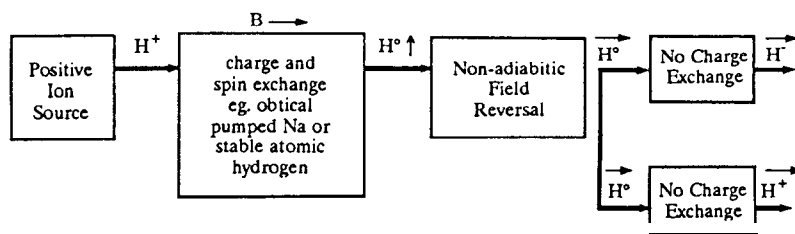
- (1) PROTONS [POS.IONS] ARE OBTAINED FROM DUOPLASMATRON SOURCE.
- (2) CESIUM CHARGE EXCHANGE CANAL CONVERTS 10 TO 20% IONS INTO METASTABLE  $2S\ 1/2$  STATE.
- (3) THE METASTABLE BEAM IS POLARISED BY STATIC FIELDS IN CONJUNCTION WITH RF. FIELDS WHICH INDUCE TRANSITION.  
 $2S\ 1/2 \rightarrow 2P\ 1/2 \rightarrow$  SPONTANIOUSLY DECAYS TO  $1S\ 1/2$  (g.s.)
- (4) POLARISED METASTABLE BEAM IS IONISED IN PREFERENCE TO G.S. BEAM BY A SELECTIVE IONIZER
- (5) ARGON GAS PRODUCES "NEGATIVE IONS" AND IODINE VAPOUR PRODUCES "POSTIVE IONS" .

FIG. 7. Schematic diagram of Lamb shift polarized source.

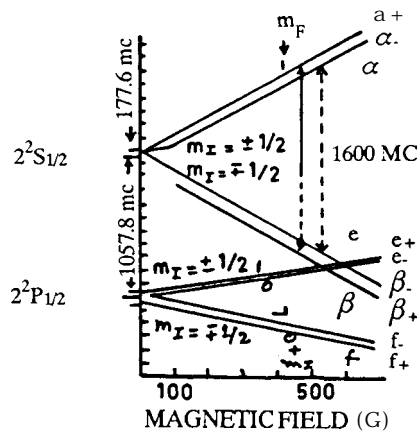
at tandem accelerators and cyclotrons for over a decade. During this time the design has been optimized in nearly all components, but the progress in the last five years has been slow. The collective world wide experience gained from Lamb-shift source laboratories indicates strongly that there is a fundamental current limit which applies to all such sources. Besides losses from space-charge quenching and collisional quenching in the production of the metastable beam, the beam divergence from the unpolarized positive ion source is found to be another limiting factor. This brightness problems of the 500 eV ( $H^+$ ) or 1 keV ( $D^+$ ) sources as well as the quenching problem limit the present polarized source out put to a maximum current of about  $3\mu A$ .

### V-3. Production of Polarized Atoms by Spin Exchange Collisions (Optically Pumped Sources)

In 1979 Witteveen<sup>28</sup> had proposed a new scheme for the ion polarization by picking up or exchanging a polarized electron when crossing an electron-polarized atomic beam. This interesting scheme of the spin exchange for a polarized ion source is shown in Fig. 8. Unpolarized positive ions, preferably produced in a ECR ion source pass through a target cell filled with a



(A) SCHEMATIC DIAGRAM OF THE PRODUCTION OF POLARIZED HYDROGEN ATOMS AND IONS BY SPIN EXCHANGE COLLISIONS (OPTICALLY PUMPED SOURCE)



(B) ZEEMAN DIAGRAM OF THE  $\sigma = 1/2$  LEVELS IN HYDROGEN  $n = 2$  INCLUDING HYPER FINE STRUCTURE

FIG. 8. Schematic diagram of optically pumped polarized source.

vapour or gas of electron spin polarized atoms. The protons pick-up a polarized electron in a charge exchange process. The spin exchange has to be carried out in a strong magnetic field  $B \geq T$  in order to prevent depolarization from atoms formed in an excited state. The neutral electron polarized hydrogen beam is nuclear polarized by inducing a transition between Zeeman states in a non-adiabatic field passage. Positive ions are produced by charge changing the atomic hydrogen beam in a neon cell. For negative ion production, an alkali or alkaline earth vapour (e.g. sodium) is used as an additional electron donor. This method can be used to polarize many kinds of ions with beam intensities which are expected to be high. The polarized proton beam is obtained by using electron polarized sodium atoms. The polarization of sodium beam is achieved by Stern-Gerlach separation. Alternately the electron donor can also be polarized by optical pumping. This scheme requires for the ions of the primary beam an even number of electrons, such that the transferred polarized electron cannot couple with another electron. This condition can be overcome by adding or subtracting one or more electrons. This interesting technique is of great value for the future development of all kinds of polarized ion

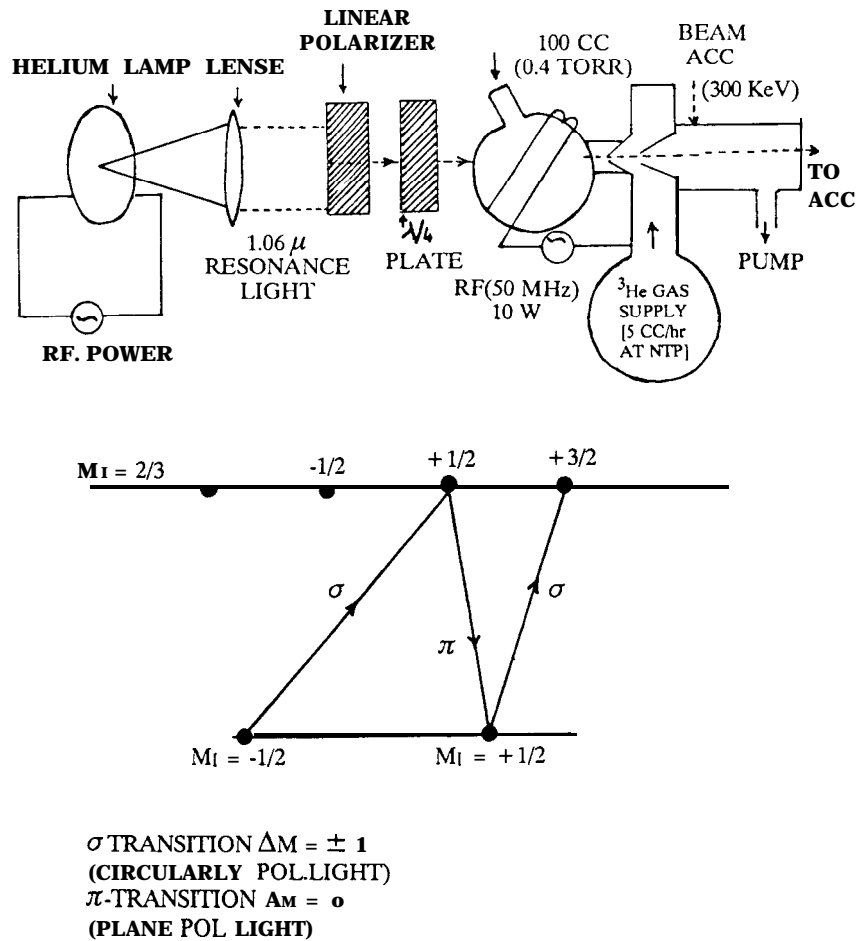
beams.

A polarized negative ion source based on an optically pumped sodium target using a single frequency dye laser has been operational for several years at the KEK synchrotron.<sup>24-26</sup> Mori et al<sup>24-26</sup> have reported a polarization of  $\cong 80\%$  for  $10 \mu\text{A H}^-$  beam and about 40% polarization for a beam intensity of  $25 \mu\text{A}$ . Similar projects are under investigation in Vancouver and Los Alamos.<sup>23</sup> At the institute for Nuclear Research in Moscow, a duoplasmatron and neutralizing gas replace the positive ion source in Fig. 8. The neutral hydrogen atoms with an energy of 5 KeV are then brought into the magnetic field surrounding the polarized sodium target where they are first reionized in Helium gas prior to the attachment of polarized electron from the sodium. The pulsed solenoid can be operated at fields upto 1.6T and a pulse width of  $30 \mu\text{S}$  with a repetition rate of 1 HZ. A peak intensity of the pulse at 1 mA has been reported by Zelenskii et al<sup>29</sup> for protons with a polarization of 65%. Polarize  $\text{H}^-$  pulses with a peak intensity of  $60 \mu\text{A}$  have been observed by Schemor.<sup>30</sup> Recently Anderson et al<sup>31</sup> has made an interesting suggestion to use a thick polarized target (electron spin polarization Na, Cs or hydrogen target thickness in  $10^{17}$  atoms  $\text{cm}^{-2}$ ) and low magnetic field in the collision region. In this case the electron and nuclear spins are coupled together by the hyperfine interaction to form a total angular momentum 'F'. This requires a field B much less than the critical field  $B_c$ . A fast unpolarized hydrogen ion captures a fast polarized electron either in a pure or a mixed state (e.g state 1 and 2 or state 3 and 4). In the mixed state hyperfine interaction mixes spins, converting some of the electron spin polarization into nuclear spin polarization. The  $\text{H}^0$  atoms in the pure state cannot capture a second electron from the polarized target to form an  $\text{H}^-$  ion source since the only bound state occurs with electron spin anti-parallel. However, the  $\text{H}^0$  atoms in the mixed states can form  $\text{H}^-$  ions by electron attachment. Since either electron may be detached in a subsequent collision, the repeated attachment of a polarized electron followed by detachment result in the entire beam being collisionally pumped into the pure state. For this, there is the necessary condition that the collision frequency be much less than the hyperfine frequency (0.3-1.5 G Hz). The problems of producing the high intensity polarized hydrogen beams by collisional pumping are presently being investigated at the Lawrence Berkeley Laboratory.

A schematic diagram of polarized  $^3\text{He}$  source at Rice university<sup>32</sup> and optically pumped<sup>24</sup> Na atomic beam source<sup>25</sup> are shown in Fig. 9 and 10 respectively.

## VI. POLARIZED NEGATIVE ION SOURCES

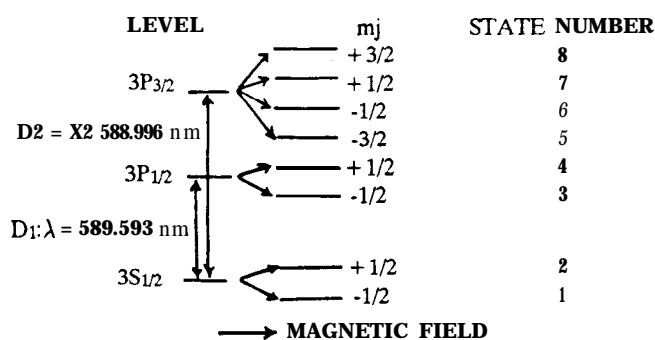
In 1982 Princeton group<sup>33</sup> had suggested that the great benefits can be expected by the injection of polarized hydrogen ions into fusion reactors. The modern particle accelerator system take advantage of the injection of negative ions in order to produce high beam intensities in the experimental area. Traditionally tandem electrostatic accelerators require the injection of negative ions. The ease with which accelerated negative ions can be extracted from cyclotrons

FIG. 9. Polarized  $^3\text{He}$  ion source.

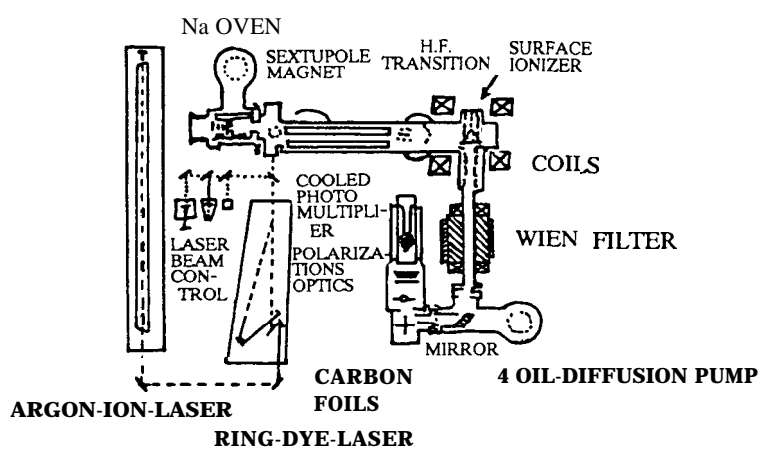
by stripping the electrons in a thin foil, makes the production of negative ions also very attractive for these types of machines. For these reasons the production of intense beams of polarized negative hydrogen ion is important for polarization experiments, which are able to investigate methodically even tiny effects in nuclear and particle physics reflecting for example the violation of symmetry laws. The different methods for the production of  $\text{H}^-$  or  $\text{D}^-$  ions had been extensively discussed in a review paper by Gruebler et al.<sup>34</sup> The following two methods are summarised in the proceeding paras.

#### VI-1. Alkali Charge Exchanger with LSPIS

Since the invention of the Lamb-shift sources this method has been used in most tandem laboratories to produce negative hydrogen ion. This device has a conversion efficiency of 30%



(A) ZEEMAN SPLITTING LEVELS OF SODIUM 3S AND 3P STATES

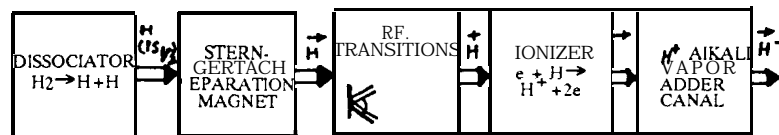
(B) EXPERIMENTAL SET-UP FOR THE OPTICAL PUMPING OF A  $^{23}\text{Na}$  ATOMIC BEAMFIG. 10. Experimental set up of optically pumped  $^{23}\text{Na}$  Atomic beam source.

for Cs as donor while sodium vapour yields 12% of  $\text{D}^-$  or 9%  $\text{H}^-$  ions. Due to the geometrical dimensions as the exchange canal only  $1/3$  of the available positive ions can effectively be used. This method of charge exchange with LSPIS has given negative ion current output of  $1 \mu\text{A}$ .

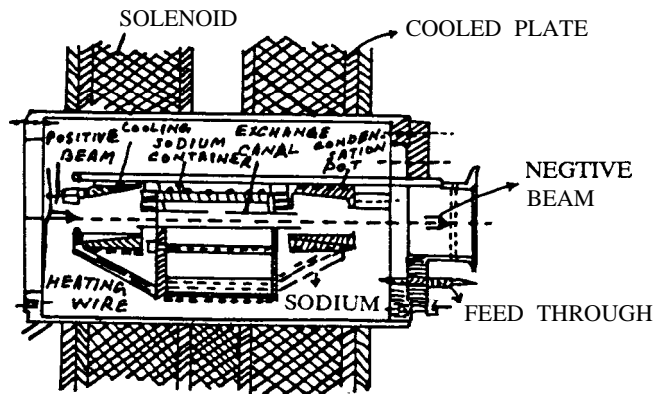
#### VI-2. Production of Polarized Negative Ions by Atomic Beam Source and Double Charge Exchange in Alkali Vapour

Recently it has been rediscovered in the many laboratories that the atomic beam sources have merits of: (i) very stable and reliable operation, (ii) the ease with which the sign of the polarization can be changed, (iii) the simplicity to choose different polarization states for deuterium. Hence, an improved ground state atomic beam polarized ion source is believed to

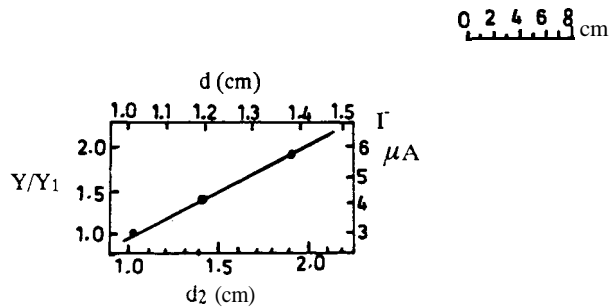
be one of the most promising methods in the production of intense beams of polarized negative ions. Such a source has been described by Gruebler et al.<sup>35</sup> A schematic diagram of this source is shown in Fig. 11(a). Hydrogen atoms are generated by dissociating molecules at low pressure in a rf discharge. An atomic beam of thermal velocity is formed by a nozzle. This beam is polarized in passing through an inhomogeneous magnetic field inducing stern Gerlach separation of the different states of the hydrogen atoms. RF transitions between the hf states of the atoms provide different nuclear polarization state. Positive ions are produced by electron bombardment of the neutral atomic beam. Negatively charged hydrogen ions are obtained by double charge exchange by passing the positive beam through a canal containing alkali vapour. In the



(A) SCHEMATIC DIAGRAM OF THE ATOMIC BEAM SOURCE FOR POLARIZED NEGATIVE HYDROGEN IONS



(B) CROSS-SECTION OF THE DOUBLE CHARGE EXCHANGE DEVICE



(C) RELATIVE YIELD  $Y/Y_1$  OF POLARIZED NEGATIVE HYDROGEN IONS AS A FUNCTION OF THE CHARGE EXCHANGE CANAL DIAMETER

FIG. 11. Polarized Negative Ion source.

ETH polarized ion source for incident ion energy of 5 keV, 100  $\mu\text{A}$  polarized positive hydrogen ion and 3  $\mu\text{A}$  of negative ions have been obtained.

Several design considerations have to be taken into account for the construction of a charge exchange device. The exchange efficiency is strongly dependent on the velocity of the positive ions entering the exchange canal. Since the high efficiency electron impact ionizer requires a high extraction voltage (15 keV) the positive ions have to be decelerated to low energy to obtain the full benefit of the charge exchange. In the case of Ca this energy is 0.5 to 1 keV, the beam is blown up and space charge problem becomes serious. The sodium vapours can be used at 5 keV. But, we have to restrict the diameter of the exchange canal ( $\approx 1$  cm) to limit the loss of sodium and to avoid the contamination of the ionizer and acceleration tube by the sodium vapour. A large sodium storage container and the use of a recirculation system would give the long operational periods without maintenance. Further, the charge exchange has to be carried out in a strong magnetic field to prevent depolarization of hydrogen atoms. These considerations have led to the design as shown in Fig. 11(b). The sodium container is placed in the centre and is maintained at 280° C. The charge exchange tube is located eccentrically in the oven and is fed with sodium vapour from a central opening. The conductance of this tube prevents an exaggerated loss of sodium. Sodium vapour leaving the canal is caught at both ends in condensation pots which are held at 150° C by a contained heating and cooling system. Provisions have been that the liquid sodium collected in these pots flows back to the central container. The investigation of the intensity as a function of the exchange canal diameter has been carried out from 1.0 to 1.4 cm. It is observed that resulting yield of polarized negative ions has a linear increase with  $d^2$  as shown in Fig. 11(c). The amount of sodium leaving the charge exchange channel is about 250 mg/h of which 80% is collected in the pots at the ends of the device. Beam intensities of 6  $\mu\text{A}$  were obtained before the acceleration and 2-3  $\mu\text{A}$  on the targets and the deuteron polarization is 90% and proton polarization lies between 75% and 80%.

### VI-3. Colliding Beam Source

This method is based on the direct charge transfer between polarized hydrogen atoms and fast atoms or ions, which act as the donor of electrons. A variety of reactions can be used in this way to produce polarized negative ions. The most advanced method takes the reaction:



Such an operational source was first developed at Wisconsin.<sup>36</sup> Schematic diagram of the colliding beam source is shown in Fig. 12. The polarized hydrogen atoms are produced in a conventional atomic beam source. After which a compressor sextupole field is used. The fast neutral Cs<sup>0</sup> beam is obtained by accelerating a Cs<sup>+</sup> ion beam from a tungsten surface ionizer to about 40 keV, and neutralizing this Cs<sup>+</sup> beam by charge exchange in a Cs vapour cell. A pair of deflection plates removes the small fraction of about 10 to 20% Cs<sup>+</sup> ions remaining after the

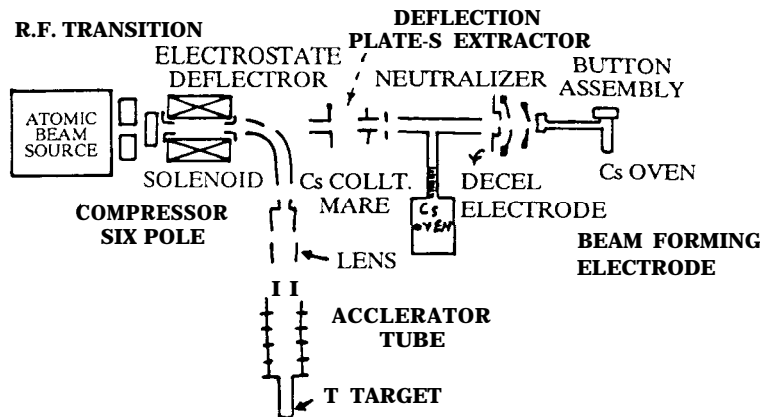


FIG. 12. Colliding beam polarized ion source.

neutralizer. The negative hydrogen ions are formed by the interaction between the  $H^0$  beam and  $Cs^+$  beam. This ionization region is located inside a 40 cm long solenoid and it is defined by two electrodes, which are biased such that the negative ions are extracted in the direction of the incoming  $Cs^+$  beam. The extraction from the collision region is supported by a stainless steel spiral which provides an axial uniform electric field. A double focussing electrostatic deflector bends the 20 keV polarized negative ion beam by  $90^\circ$  in the acceleration tube. A hole in the outer electrode of this device permits the entry of the  $Cs^+$  beam in the ionizer. The maximum polarized beam, intensity so far observed is about  $3 \mu A$  for both  $H^-$  and  $D^-$  ions.

## VII. POLARIZED HEAVY ION SOURCES

A very interesting field in ion technology is the development of polarized heavy ion sources. A selected list of heavy ions which possibly could be polarized by the atomic beam method using surface ionization is given in the Table III. The polarized heavy ions are very much interesting in nuclear physics due to the under mentioned reasons: (i) that the spin-dependent part in the nuclear interaction can be investigated with polarized ions; (ii) for ions with  $I \geq 1$  having the static ground state deformation a "Shape effect" appears due to the projectile shape. This effect would be more dominant for aligned deformed heavy ions; (iii) In a spin aligned beam the quadrupole moments of the mass and charge distribution are also aligned. The use of spin precessor after ion source can give any desired direction to the spin axis. Hence the symmetry axis of the mass and charged distribution could be changed; (iv) The heavy ion interaction is very sensitive to the interaction distance. Using aligned deformed heavy ions, this critical distance can be changed just by turning the alignment axis; (v) The  $^7Li$  and  $^{23}Na$  ions have strong deviations from spherical-shape. Hence, they are the most interesting to study shape effects.

TABLE III. List of heavy ions which can be produced by the atomic beam method and surface ionization.

Element Z	Isotope	Abundance %	Ionization energy (eV)	Electron affinity (eV)	Nuclear spin	Bcrit(mT)	Surface	Ionization Efficiency of ion (max. %)	Charge
Electronic Structure: $^2S_{1/2}$ , electronic spin 1/2									
3	6Li	7	5.4	0.61	1	8.2	w-o	100	+
	7Li	93	5.4	0.61	3/2	28.8	w-o	100	+
11	23Na	100	5.1	0.54	3/2	633	w-o	100	+
	39K	93	4.3	0.50	3/2	16.5	w-o	100	+
19	41K	7	4.3	0.50	3/2	9.1	w-o	100	+
37	85Rb	100	4.2	0.49	5/2	10.8			+
55	$^{133}\text{Cs}$	100	3.9	0.47	7/2	328	w-o	1-00	+
Electronic Structure: $^2P_{1/2}$ , electronic spin 1/2									
49	$^{113}\text{In}$	4	5.8	70	9/2	12019	Ir/W-O	40/>90	+
	$^{115}\text{In}$	96	5.8	0.7/0.2	9/2	12021	Ir/W-O	40/>90	+
Electronic Structure: $^2D_{3/2}$ , electronic spin 3/2									
71	$^{125}\text{Lu}$	97	5.4		7n	56.5			+
Electronic Structure: $^2P_{3/2}$ , electronic spin 3/2									
9	$^{19}\text{F}$	100	17.4	4.1	1/2	71.7			
	$^{35}\text{Cl}$	75	13.8	3.8	3/2	21.0	W-TwW-0-Ca	2.6/50	-
17	$^{37}\text{Cl}$	25	13.0	3.8	3/2	17.5	W-Tn/W-O-Ca	2.6/50	-
35	$^{79}\text{Br}$	50	11.8	3.6	3/2	102	W-Tn	0.4	-
	$^{81}\text{Br}$	50	11.8	3.6	3/2	108	W-Tn	0.4	-
53	$^{127}\text{I}$	100	10.5	3.1	5/2	124	W-Tn	0.3	-

Due to above reasons, the heavy ion polarized sources have been developed at Heidelberg<sup>37-38</sup> and Dersbury.<sup>39</sup> We summarize the main features of these sources. The basic configuration of the source is shown in Fig. 13. A polarized atomic beam is produced by an oven, a Stern-Gerlach magnet and a system of hf transitions and this is ionized to positive ions on a hot tungsten surface. The ionizer is operated in the transverse guide field of a dipole magnet. The beam is extracted upward and focussed by 90° spherical electrostatic deflector into the charge exchange canal. The negative ions beam is then passed through a Wien Filter, where the desired spin direction is set, and injected into the preaccelerator tube.

A schematic diagram of the Heidelberg-Dersbury polarized heavy ion source is shown in Fig. 14. The description of basic units is given below:

#### VII-1. The Sodium Oven

The sodium oven consists of an evaporation cylinder and a collimator chamber and is of the re-circulating type. Two heater cartridges in a copper jacket keep the cylinder temperature at 500° C while the collimator temperature is maintained around 140° C which allows the Na Vapour to condense and the liquid to be directed back into the cylinder. The atomic beam is formed by 1.5 mm holes in the cylinder. The collimator beam has a density of upto  $7 \times 10^{17}$

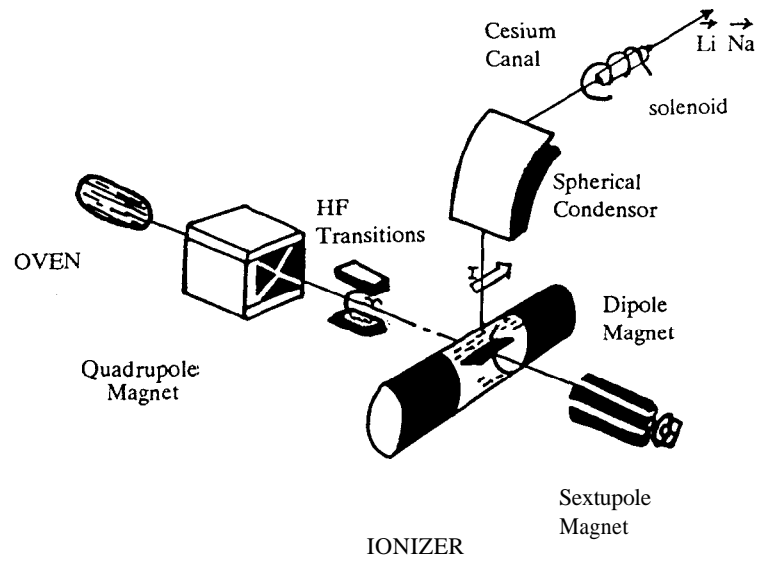


FIG. 13. Configuration of Heavy Ion polarized source.

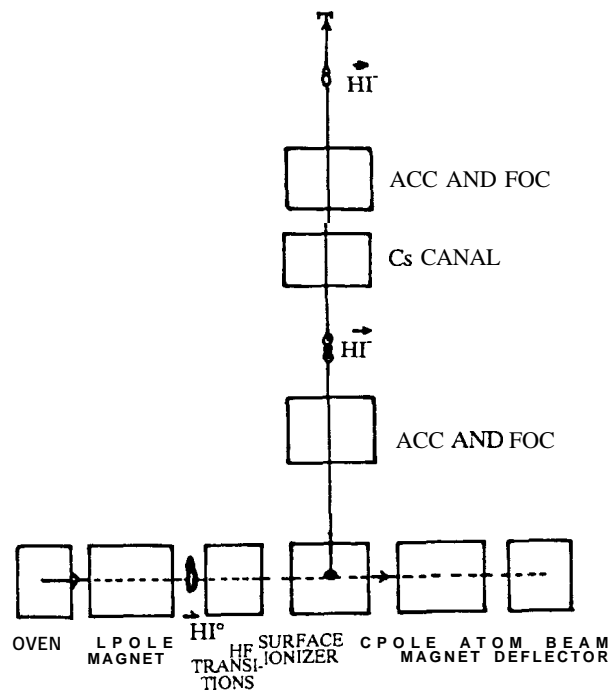


FIG. 14. Schematic diagram of polarized heavy ion source.

particles/S. Sr as measured by a small ionizer directly behind the oven gate. The oven is filled with sodium and serviced in a glove box which has an inert argon atmosphere.

### VII-2. Stern-Gerlach, Separation Magnet

For the Stern-Gerlach separation a quadrupole magnet is chosen. The magnet length is 38 cm. The pole tips, pole pieces and the yoke of the magnet are manufactured from Armico iron. The gap between the pole tips is 11 mm and the shape of the pole tips is optimized to obtain the maximum field strength (23.5 KG) in the gap. The coils (each 26 turns) are made from copper tube (I.D. = 4 mm and O.D. = 6 mm) insulated by fiberglass and impregnated with Araldite. The magnetic field at the pole tips saturates around 16 KG at  $\approx 180$  A. The total power consumption is 1.5 KW and the pressure in the magnet chamber is of the order of  $10^{-7}$  torr.

### VII-3. The RF Transitions

The rf transitions units are installed around a glass tube (30 cm long and 14 mm inside diameter) connecting the quadrupole magnet and the ionizer vessel. The weak field transition (WFT) produces the vector polarization at  $\approx 10$  MHz whilst the strong field transitions (SFT) produce the tensor polarization  $\approx 2$  GHz. In both cases the oscillator signal is amplified in externally controlled power amplifiers before being fed into the resonators. Two  $\sigma$  transitions between  $4 \rightarrow 6$  and  $2 \rightarrow 8$  levels on the Breit-Rabi diagram (Fig. 15) are employed in SFT. The

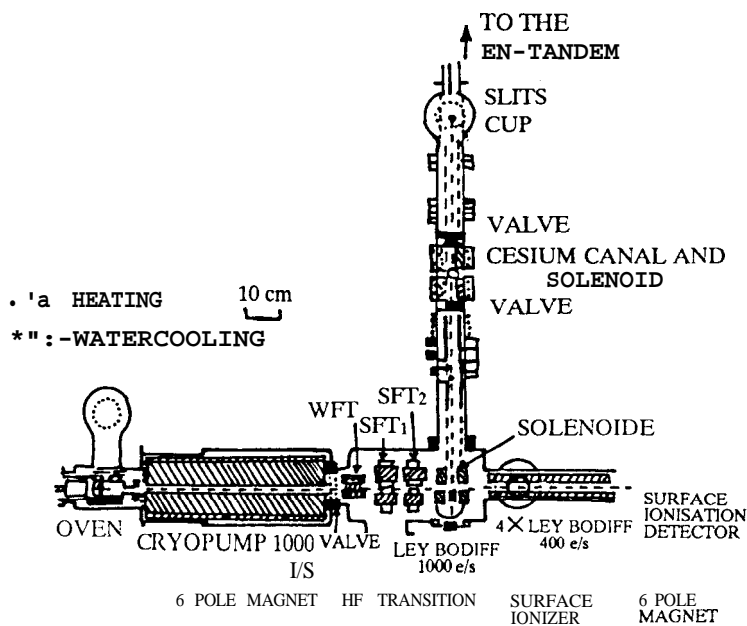


FIG. 15. Polarized heavy ion source in more detail.

setting of both the gradient and static magnetic fields in the transition region is checked by observing if there is about 25% decrease in the current monitored in the small ionizer sited along the atomic beam line behind the sextupole magnet.

#### VII-4. The **Ionizer Assembly**

The atomic beam is ionized on a tungsten strip (10 mm wide and 50  $\mu\text{m}$  thick) which is tilted at  $45^\circ$  to the beam axis. It is heated by an ac current of more than 50A to about 1800 K. The ionizer is operated at +4KV for lithium and + 12 to 16 KV for sodium to obtain the optimum energy for the charge exchange in cesium vapour. A dipole magnet with 10 cm diameter pole tips and 12 cm gap provides a strong magnetic field to define the spin symmetry axis during ionisation. The ionizer filament (strip) can be remotely moved out of the atomic beam path when setting the rf transitions. The strip temperature is deduced by the pyrometer. The positive ions are extracted from the surface of strip by a grid (90% transparency). Then the positive beam is deflected and focused into the charge exchange canal by a spherical condenser of mean radius 20 cm and 4 cm gap. The electrodes are manufactured from cast red brass rings and hard chromium plated. The deflection voltages of  $\pm 1$  to  $\pm 2$  keV are used. A Faraday cup is inserted at the object point of the condenser to optimise the setting of the extraction system.

#### VII-5. The **Charge Exchange Unit**

The extracted beam from the ionizer is brought onto the axis of the injection line by a 90 spherical condenser which has a focus in the middle of the 18 cm long and 10 mm diameter canal of the charge-exchange unit. The canal is of the wick type and is mounted in the bore of a solenoid which produces a guiding field of upto 1.5 KG along the direction of the beam. About 5g of cesium, transported in the liquid state by argon pressure from a heated external reservoir, is kept in the canal central cavity. The canal is heated to 140 to 150° C for an optimum yield of the negative fraction. The canal ends are kept at 35° C to condense the Cs vapours. The resulting liquid Cs is fed back to the canal centre by the capillary action of a fine mesh lining the walls. Cooled copper plates around the canal ends prevent the escape of Cs from the unit. The Cs vapour density is monitored by a small ionizer behind the spherical condenser. The charge exchange unit is electrically insulated allowing the canal to be operated at a potential of upto 6 KV. The effective charge-exchange efficiency (the ratio of the negative and positive currents) at  $E_{\text{Na}} = 18 \text{ KeV}$  is about 3%.

#### VII-6. The **Wien Filter (W.F. Assembly)**

The Wien filter is used to precess the spin from the original direction parallel to the beam axis into any desired direction. The Wien filter is rotatable around the beam axis. It has a magnet of 38 cm long with a 5 cm gap. The electrodes are mounted in a rectangular vacuum pipe.

The optimum transmission through the Wien filter is checked by inserting a third Faraday Cup. The asymmetry ( $\epsilon_c$ ) in the photon counting rate of circularly polarized light depends on the angle between the spin symmetry vector rotating in the WF magnetic field and the direction of photon emission as

$$\epsilon_c = T_{10}t_{10} \cos \phi + T_{20}t_{20}(3 \cos^2 \phi - 1)$$

For linearly polarized light,  $\phi = 90^\circ$  we get the asymmetry as:

$$\epsilon_L = T_{20}t_{20}(3 \cos^2 \psi - 1)$$

Where  $\psi$  is the angle between the spin symmetry vector and the transmission direction of the linear polarizer.

For Daresbury source<sup>39</sup> the beam intensities upto  $40 \mu A$  have been measured in first Faraday cup i.e. after the ionizer. The maximum vector polarization is close to the theoretical value of  $t_{10} = \sqrt{9/20} = 3/2\sqrt{5}$ .

### VIII. PERFORMANCE OF THE PIS

In the early stages of PIS development, the main stress was on the high beam current and the polarization while the importance of the beam quality was not sufficiently appreciated. But, in order to assess the quality of PIS; We have to compare the following parameters.

#### VIII-1. Figure of Merit of PIS

It is  $I.P^2$  (I is intensity and P is polarization produced). The higher value of  $I.P^2$  is interesting for the experiments. The value of figure of merit is shown in Table I for polarized deuterium beams.

#### VIII-2. Emittance of Polarized Beams

An elaborate ion optics for the injection path are needed in order to prevent a mismatch of the emittance of the beam with the acceptance of the accelerator. According to Ohlsen et al,<sup>40</sup> the ionization or neutralization of a beam in a homogenous longitudinal magnetic field will increase the emittance of the beam on passing the stray field in a charged state. When the radius of the beam in this region is R and the applied longitudinal magnetic field is B then the emittance increase will be proportional to  $B.R.^2$  For given atoms, the magnetic field B is determined by their critical field. Therefore, the beam optics should be designed such that a waist is formed in the fringing field region. In general, the emittance increases with higher fields as given below:

Field	Emittance (mm mrad. (MeV) <sup>1/2</sup> )
30 G	$2\pi$
300 G	$5\pi$
1000 G (1 KG)	$11\pi$
75 KG	$20\pi$

The above data show that the emittances of the beam even for very high field ionizer is within reasonable limits with a well designed extraction and focussing system at the exit of the solenoid e.g. the acceptance of the tandem accelerator is about  $12\pi$ .

### VIII-3. Spin Reversal

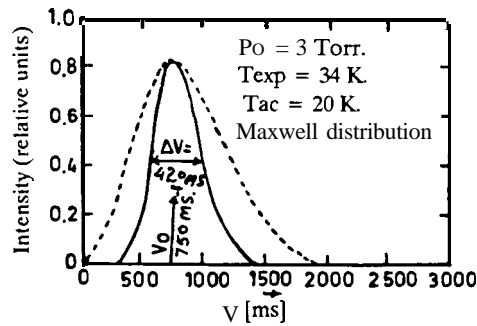
In using a polarized beams after the acceleration for nuclear physics experiment the beam properties which allow the application of high precision measuring techniques are as important as beam intensity and beam polarization. One of the most important features is the reversal of the spin direction of the change of the sign of the polarization without synchronized modulation of the beam intensity, polarization and displacement. In principle, the spin can be flipped by reversing the E and B fields of the spin precessor (Wien filter). This crude method has inherent ion optical problems which induce steering effects, strong intensity and displacement modulation on the target as well as the disadvantage that a rapid reversal is excluded.

In an atomic beam source the spin slip can easily be achieved by switching the selected RF transitions in the neutral beam. For protons,  $2 \rightarrow 4$  transition followed by a weak field transition can change  $P_z$  from +1 to -1 if two transitions are switched on and off alternatively. By using different possible modes it is possible to produce a pure vector polarization with different sign or a mixed vector and tensor polarization. But, this method requires carefully turned RF transitions. In Lamb-shift sources the proper alternating spin reversal is more difficult since small magnetic transverse fields in front of the argon region must be turned on and off.

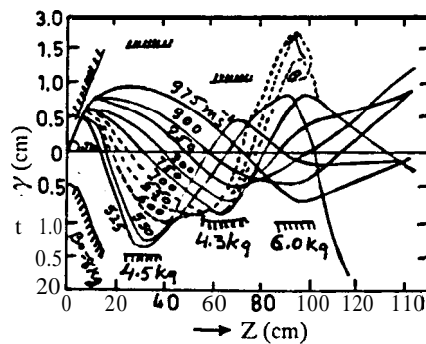
## IX. POSSIBLE FUTURE IMPROVEMENTS

The prospects for further improvements for all types of polarized ion sources are encouraging. For conventional atomic beam sources the positive ion currents have attained impressive large values but still additional improvements can be achieved; while for Lamb-shift sources we need new ideas to over-come the space-charge and the quenching problems. The production of the polarized heavy-ions and negative ions have not been optimised so far. Thus, we would like to mention the possible future improvements in brief.

(i) Reduction of self scattering of the beam: The measurements on the velocity distribution made on the atomic and molecular beams indicate that the velocity distribution is not exactly Maxwellian as shown in Fig. 16. Since the probability of the particles emerging from an aper-



(a) The velocity distribution of an atomic hydrogen beam measured at the ETH atomic beam apparatus. Temperature of the accomodator 20K. Pressure in the dissociator  $P_0 = 3$  Torr.



(b) Calculated Trajectories between 525 and 975  $\text{m s}^{-1}$  and an angle of  $5^\circ$  from the axis. The plot gives the radial distance of the atoms from the symmetry axis of the magnets.

FIG. 16. Velocity distribution of an atomic beam.

ture is proportional to the particle velocity; the velocity distribution in a beam shows that the most of the particles in beam move with less velocity than the average velocity of the Maxwellian distribution. Singh<sup>41</sup> had investigated that the scattering between atoms of lower and higher velocities in the beam reduces the beam intensity inversely with distance. It was found that the self scattering of an atomic beam can play an important role in the construction of PIS. It had been suggested that the use of the specially Shaped beam separator (peeler/skimmer) can have a great effect on the beam intensity of the PIS. It is possible to improve the beam intensity by using the peelers of the shape as shown Fig. 17, between the dissociator and sextupole. The practical use of such peeler was tested experimentally at Birmingham PDS.<sup>41</sup>

(ii) Reduction in drift space: The shorter drift space from the nozzle (atomic effusion) to the sextupole entrance would improve the solid angle of the acceptance by the sextupole and

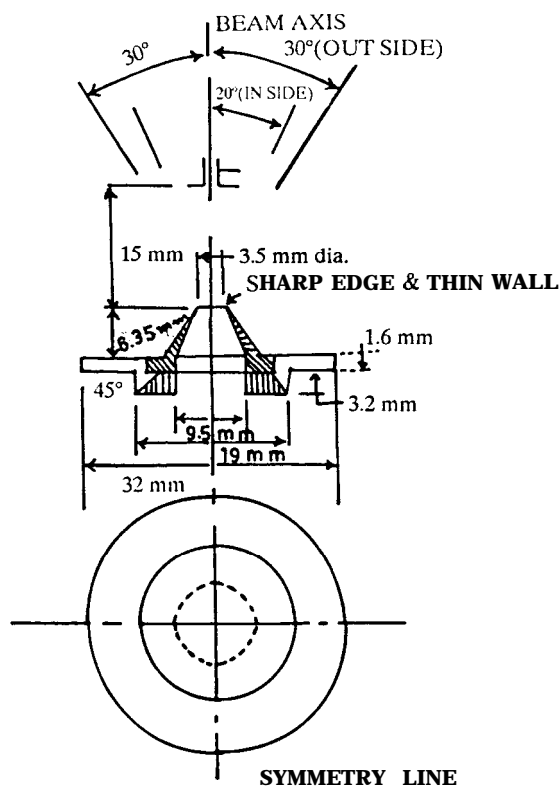


FIG. 17. The drawing of the peeler.

reduce the background gas scattering which decreases the beam intensity by a factor of  $\exp(-l \cdot p)$ .

(iii) The use of multimagnet system: The use of multimagnet systems for the separation and focussing of electronic states of an atomic beam would allow a high flexibility in the nuclear polarization and polarization reversal by selecting single states. A single Zeeman state can be separated by the use of two Stern-Gerlach sextupole magnets with an intermediate RF transitions as shown in Fig. 18. The addition of the second sextupole would also help to optimize the focussing into the ionizer.

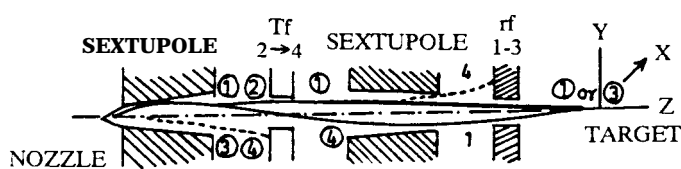


FIG. 18. Production scheme for single substates.

(iv) Cooling of the Atomic Beam: The density of the atomic beam is inversely proportional to the most probable velocity i.e. to  $T^{-1/2}$  and the solid angle of acceptance by a sextupole magnet is proportional to  $T^{-1}$  (where  $T$  is the absolute temperature of the dissociator). Therefore, the density of an atomic beam after the sextupole magnet is strongly dependent on the temperature as  $T^{-3/2}$ . Hence the cooling of the dissociator to low temperature may lead to a substantial improvement in the intensity of the ground state atomic beam source. The density gain factor is 7.5, 57 and 590 for the liquid nitrogen, liquid hydrogen and liquid Helium-4 respectively as compared with room temperature. These density gains can only be realized if there is no intensity loss from the dissociator due to the cooling and if the geometry of the beam forming apertures and the separation magnets are adjusted adequately. The several attempts have been made to cool atoms in the beam forming stage at Bonn,<sup>42</sup> Argonne<sup>43</sup> (ANL), Zürich<sup>44</sup> (ETH) and BNL.<sup>45</sup> The experimental set up for the production of cooled high density atomic hydrogen beams built at ETH is shown in Fig. 19. These investigations have been carried out for judging the efficiency of the cooling, the properties of the beam forming elements and the degree of dissociation obtained in the atomic beam. In future the better results could be obtained if the further investigations are carried out for the optimization of thermal accommodations, recombination and beam formation at low temperatures.

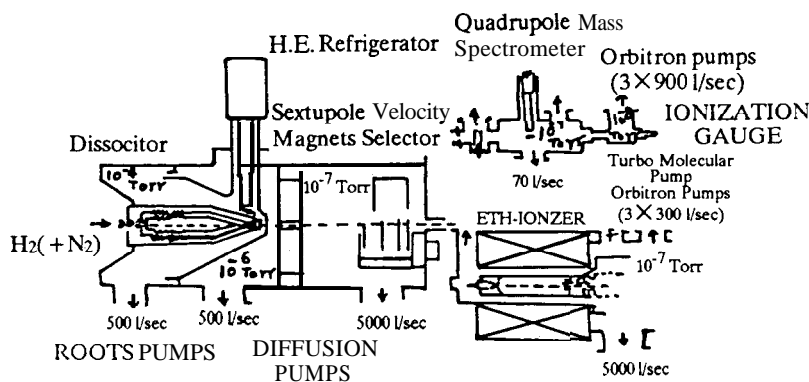


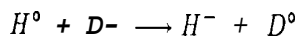
FIG. 19. ETH experimental arrangement for cooling a high density atomic beam.

(v) ECR Ionizer: The use of electron cyclotron resonance (ECR) ionizer as investigated by Clegg et al<sup>46</sup> could give the better results for ionization of light and heavy ions. In this type of ionizer a plasma of cold ions with hot electron is produced in the ionization region. The applied electron cyclotron resonance conditions produce a high electron density which can be  $10^3$  times higher than in a normal electron impact ionizer. Electron energy of several KeV can be obtained. Although this method gives better results but further investigations are required to study possible depolarization effect in ECR ionizer.

(vi) For the production of polarized positive ions, the use of photoionization as proposed by de Jong<sup>47</sup> could increase the current output by a large amount. But it requires further investigations.

(vii) The investigation of charge exchange in alkaline earths by McFarland et al<sup>48</sup> shows that these vapours can yield negative ions upto 50%. A substantial improvement of the negative ion beam intensity can be expected by the use of a more efficient charge exchange medium and the combination of charge exchange device and ionizer into a single unit. For such a low energy double charge exchanger detailed investigations are needed in order to finalize the technical design.

(viii) It has been speculated by Allesen<sup>49</sup> that the higher yields of the polarized negative ions could be obtained from the charge-transfer reaction.



The cross-section for this process is about 5 times larger than with Cs. The required high current of unpolarized D<sup>-</sup> beams can be generated from the surface plasma ion sources. This method seems most promising but the difficulty of the method arises due to space charge effects.

(ix) A very interesting development in the polarization of neutral beams is possible by exciting the atomic states with lasers of sufficient power as shown in Fig. 3 for <sup>23</sup>Na. It is seen that the optical pumping can replace the Stern-Gerlach separation. Since it would reduce the distance between the beam forming device and the ionizer to a few cm, the sustained solid angle is very large. Hence, an improvement in the beam intensity may be expected. Recently developed an optically pumped polarized ion sources for LAMPF has been described by York et al.<sup>23</sup>

(x) For circular machines with faster time structure a substantial intensity increase can be gained at the target by bunching the beam in the injection path. The bunching is highly recommended for the fast pulsed polarized beams which are used to produce the polarized neutrons.

(xi) The pulsed operation of an atomic beam source promises substantial increases in the beam current in the future. For accelerators with low duty cycle (synchrotrons) it is possible to operate the dissociator in a pulsed mode and enjoy the benefit of a factor of 2 to 3 enhancement in the beam current.

(xii) The magnetic separation of a fast neutral beam using a cryogenic sextupole followed by direct conversion to ions using charge exchange is also food for future thought and development of polarized ion sources.

## X. CONCLUSION

It is seen that the different types of operational polarized ion sources exist. This variety makes it sometimes difficult to decide in which direction one should proceed. One should keep

in mind that the realization of technical progress is tedious and sometimes frustrating compared to the satisfaction that the creation of new ideas can generate. The prospects for further improvements for all types of polarized ion sources are encouraging. It seems entirely likely that in the not too distant future, nuclear physicists will have the opportunity of working with polarized beams of intensity comparable to that of unpolarized beams.

The performance of the existing optically pumped polarized ion sources after only 5 years of development is truly remarkable. The source at the Institute for Nuclear Research at Moscow<sup>51</sup> has produced 150  $\mu\text{A}$  of  $\text{H}^-$  beam with polarization of 65% and 1 mA of  $\text{H}^+$  beam with polarization of 65%.

### ACKNOWLEDGMENTS

I am very grateful to all my colleagues all over the world who have provided me with the newest information about the developments in the field. I am highly indebted to Drs. W. Gruebler (Zurich); Y. Mori (KEK); O. Karban (Birmingham-NSF Daresbury) and York (Los Alamos) for prompt response to my request for the recent progress reports. I apologize for having not been able to include all information received in this talk. I would like to thank the organizing committee of First Asia Pacific conference on Atomic and Molecular Physics; Academia Sinica, Taipei; the Indian National Science Academy (INSA) and the Department of Science and Technology (DST), New Delhi for providing the financial assistance.

### REFERENCES

1. Proc. First Int. Symp. on Polarization Phenomena of Nucleons, Basel, P. Huber and K. P. Mayer, eds. Birkhauser Verlag Basel (1961).
2. Proc. Second Int. Symp. on Polarization Phenomena of Nucleons, Karlsruhe, P. Huber and H. Schopper, eds. Birkhauser Verlag Basel and Stuttgart (1966).
3. Proc. Third Int. Symp. on Polarization Phenomena in Nuclear Reactions, Madison, H. H. Barshall and W. Haeberli eds. the University of Wisconsin Press, Madison (1971).
4. Proc. Fourth Int. Symp. on Polarization Phenomena in Nuclear Reactions, Zurich, W. Gruebler and V. Konig, eds. Birkhauser Verlag Basel and Stuttgart (1976).
5. Proc. Fifth Int. Symp. on Polarization Phenomena in Nuclear Physics, Santa Fe, New Mexico, USA, G. G. Ohlsen et al, eds. A.I.P. Proc. No. 69-AIP, New York (1981).
6. Proc. Sixth Int. Symposium on Polarization Phenomena in Nuclear Physics, Osaka, M. Kondo et al, eds. Suppl. Journ. Phys. Soc. Japan 55 (1986).
7. Proc. Int. Symp. on High Energy Physics with Polarized Beams and Targets Lausanne. C. Joseph and J. Soffer eds. Birkhauser Verlag Basel (1981).
8. Proc. High Intensity Polarized Proton Source, Vancouver, 1983, G. Roy and P. Schmor eds. AIP Cons. Proc. No. 117, AIP, New York (1984).

9. Proc. Workshop on Polarized Targets in Storage Rings, Argonne, Report ANL-84-50, (1984).
10. Proc. 4th Int. Workshop on Polarized Target Material and Techniques. W. Meyer ed, physikalische. Institute, Universitat Bonn (1985).
11. Proc. Intern. Workshop on Polarized Sources and Targets, Montana (1986), S. Jaccord and S. Mango eds, Helv. Phys. **Aeta** 59:513-806, Birkhauser Verlag Base1 (1986).
12. Int. School of Fusion Reactor Technology: Muon catalyzed fusion and fusion with Polarized Nuclei, ' Ettore Majorana' , International centre for scientific culture, Erice, Italy, April 3-9 (1987).
13. Proc. High Energy Spin Physics, Brookhaven, G. M. Bunce ed. AIP Conf. Proc. No. 95, AIP New York (1983).
14. Proc. Int. Symp. on High Energy Spin Physics, Marseille, J. Soffer ed, Journ: Phys, **C2**, 46 (1985).
15. Proc. Int. Symp on High Energy Spin Physics, Profvino (USSR) 1986.
16. E. M. Henley, **Nucl Phys. A** 483,596 (1988).
17. J. W. T. Dabbs, L. D. Roberts and G. W. P. Parker **Physica** (Nether-lands) 24,869 (1958).
18. D. Pines, J. Bardeen and C. P. Slechter, Phys. Rev. 106,489, (1957).
19. C. D. Jeffries, Phys. Rev. 117, 1056 (1960).
20. A. Kastler, **Proc. Phys. Soc. A**67, 853 (1954); J. Opt. Soc. Amer. 47,460 (1957).
21. B. Cagnac, J. Brassel and A. Kastler **C. R. Acad. Sci.** **246**, 1827 (1958).
22. D. M. Hardy, S. D. Baker and W. R. Boykin **Nucl, Instr. and Meth.** **98**, 141 (1972).
23. R. L. York et al, International Workshop on Hadron Facility Technology, Los Alamos National Laboratory Report No. LA-UR-87-699.
24. Y. Mori, K. Ikegami, A Takagi and S. Fukumoto, 5th Int. Symp. on High Energy Spin Physics, BNL (1982).
25. Y. Mori, K. Ikegami, A Takagi and S. Fukumoto, **Nucl. Inst. and Meth.** 220,264 (1984).
26. Y. Mori et al, 4th Int. Symp. on the production and Neutralization of Negative Hydrogen and Beams, BNL, dct. 27-31 (1986).
27. S. D. Baker, D. H. McSherry and D. O. Findley. Phys. Rev. **178**, 1616 (1969).
28. G. J. Witteveen, **Nucl. Inst. and Meth.** **158**, 57 (1979).
29. A. N. Zelenskii et al, **Suppl. Journ. Phys. Soc. Japan** **55**, 1064 (1986).
30. P. W. Schmor, Helv. Phys. **Aeta** 59,643 (1986).
31. L. W. Anderson et al, Phys. Rev. Lett. 52,609 (1984) and J. Phys. B. At Mol. Phys 17,229 (1984).
32. D. O. Findley et al, **Nucl. Inst. and Meth.** 71,125 (1969).
33. R. M. Kulsrud, H. P. Furth, E. J. Valeo and M. Goldhaber, Princeton Plasma Physics Lab. Report 1912 (1982).
34. W. Gruebler and P. A. Schmelzleach AIP Conf. Proc. 69,848 (1981).
35. W. Gruebler et al, **Nucl. Inst. and Meth.** 186,655 (1981); 212,1 (1984).
36. D. Hennies et al, Phys. Rev. Lett. **40**, 1234 (1978).
37. E. Steffens, **Nucl. Inst. and Meth.** 184, 173 (1981).

38. D. Kramer et al, **Nucl. Inst. and Meth.** 220,123 (1984).
39. O. Karban et al, The report on " the polarized heavy ion source at the NSF in Daresbury (July 5, 1988).
40. G. G. Ohlsen et al, **Nucl. Inst. and Meth.** **73**, 45 (1969).
41. J. Singh, **Nucl. Inst. and Meth.** 99,413 (1972).
42. H. G. Mathews et al, **Nucl. Inst. Meth.** 213,155 (1983).
43. P. F. Schuttz, E. F. Porker and J. J. Madsen, **ATP Proc.** 69,909 (1981).
44. W. Gruebler, Invited Talk at the International School of Fusion Reactor Technology, **Erice**, Italy (1987).
45. A. Hershcovitch et al. **Helv. Phys. Acta** 59,526 (1986).
46. T. B. Clegg et al, **Nucl. Inst. Meth. A** 238,195 (1985).
47. De Jang, **AIP Conf. Proc.** 117,103 (1984).
48. R. H. Mcforland et al, **Phys. Rev.** **A26**, 775 (1982).
49. P. W. Alleson, **IEEE Trans. Nucl. Sci.** **24**, 1594 (1977).
50. L. W. Anderson and G. A. Nimmo, **Phys. Rev. Lett.** **42**, 1520 (1979).
51. A. N. Zelenskii et al, **Helv. Phys. Acta** 59,681 (1986).